19th IFAC Symposium on Automatic Control in Aerospace -
ACA 2013, 2-6 September 2013, Würzburg, Germany

Attitude stability analysis for an Earth pointing, magnetically controlled spacecraft

Fabio Della Rossa * **Fabio Dercole** * **Marco Lovera** *

* *Dipartimento di Elettronica, Informazione e Biongegneria, Politecnico di Milano Piazza Leonardo da Vinci 32, 20133 Milano, Italy (e-mail: {dellarossa,dercole,lovera}@elet.polimi.it).*

Abstract: The dynamics of a spacecraft equipped with magnetic actuators operating under a static attitude and rate feedback control law designed using averaging theory is considered and the asymptotic behavior of the closed-loop system as a function of the averaging scaling parameter is analysed numerically through continuation. We show that the (almost) global stability of the attitude equilibrium granted by the theory for sufficiently small scaling is lost at larger gains. Moderately chaotic fluctuating regimes appear for increasing scaling, while the attitude equilibrium maintains local stability, though with smaller and smaller basin of attraction.

1. INTRODUCTION

Attitude control design for rigid spacecraft equipped with magnetic actuators has been widely studied in recent years (see, *e.g.*, the survey paper Silani and Lovera (2005)). As is well known, the design problem is challenging due to the principle of operation of such actuators, which generate control torques by interacting with the magnetic field of the Earth. This has a number of implications which make the magnetic attitude control problem significantly different from the conventional one. First of all, such actuators cannot provide three independent control torques at each time instant. In addition, their behavior is time-varying (periodically forced), as the control mechanism hinges on the variations of the Earth magnetic field along the spacecraft orbit. Nevertheless, attitude stabilisation is possible because *on average* the system possesses strong controllability properties for a wide range of orbit inclinations (see also Bhat and Dham (2003)).

A significant effort has been dedicated in recent years to the problems of analysis and design of magnetic control laws for *local* operation of a satellite near a constant reference attitude, using mainly tools from periodic control theory exploiting the (quasi) periodic behavior of the system near an equilibrium (see, *e.g.*, Lovera et al. (2002); Psiaki (2001); Wisniewski and Stoustrup (2004); Zanchettin and Lovera (2011)).

Similarly, attention has been dedicated to *global* formulations of the problem. In Wisniewski and Blanke (1999); Damaren (2002); Arduini and Baiocco (1997) the attitude regulation problem for Earth pointing spacecraft has been addressed exploiting periodicity assumptions and resorting to passivity arguments to prove local asymptotic stabilisability of stable open-loop equilibria. In Wang and Shtessel (1998) similar arguments have been used to study a state feedback control law for the particular case of an inertially spherical spacecraft. More recently, in Lovera and Astolfi (2004) (resp. Lovera and Astolfi (2006)) almost global[1] stability conditions for state feedback control laws achieving inertial pointing (resp. Earth pointing) for magnetically actuated spacecraft have been presented. The above mentioned results concerning almost global stabilisation using magnetic actuators have been derived by resorting to averaging theory, *i.e.*, by associating to the time-varying dynamics of the magnetically controlled spacecraft a suitably defined time-averaged counterpart and showing that for sufficiently small values of a scaling parameter ε the trajectories of the former can be approximated by the ones of the latter.

This averaging technique provides an interesting characterisation of the global properties of magnetic state feedback controllers, but leaves open the problem of characterising the range of values of the scaling parameter for which the result actually holds. In Della Rossa et al. (2012) the above mentioned characterisation was carried out (using bifurcation analysis) for the case of an inertially pointing satellite and provided a number of insights into the dynamics of the controlled spacecraft. Note, in passing, that while a few analyses based on bifurcation theory for the dynamics of a rigid spacecraft immersed in a central gravitational field can be found in the literature (see, *e.g.*, Fujii et al. (2000); Kuang et al. (2002)), as far as the interaction with the geomagnetic field is concerned it appears that only the case of a spacecraft with a constant residual magnetic dipole has been studied (see Chen and Liu (2002)). Note that nonlinear analysis methods have been also applied to atmospheric flight dynamics problems, see, *e.g.*, Mehra and Prasanth (1998); Lowenberg and Menon (2007).

The aim of this paper is to investigate numerically the local and global stability of an *Earth pointing* magnetically

[1] Given a system $\dot{x} = f(x)$ we say that an equilibrium x_0 is almost globally asymptotically stable if it is locally asymptotically stable, all the trajectories of the system are bounded and the set of initial conditions giving rise to trajectories which do not converge to x_0 has zero Lebesgue measure.

actuated spacecraft operating under the state feedback control law of Lovera and Astolfi (2006), for increasing values of the scaling parameter ε. Continuation techniques (typical of numerical bifurcation analysis, see Meijer et al. (2009)) are used to analyse the Floquet multipliers of the limit cycle of the (periodically forced) system associated with the attitude equilibrium. Time is discretized using orthogonal collocation techniques (see, *e.g.*, de Boor and Swartz (1973); Ascher et al. (1995)) and, provided the resolution is sufficiently high, it is found that all multipliers remain in the unit circle for reasonable values of the scaling parameter. By studying the least stable eigenfunctions, it is further possible to characterize the perturbations that take longer to be reabsorbed, or eventually lead to alternative attractors. In this way alternative fluctuating attitude regimes characterized by positive Lyapunov exponents (chaotic attractors) can be determined. Such regimes require smaller and smaller perturbations to be reached as the control gain is increased.

The paper is organized as follows. In Section 2 the model of the system is presented, while in Section 3 the state feedback magnetic attitude control law studied in this paper is briefly described. Subsequently, in Section 4 the local analysis approach is presented and its results are discussed. Finally, in Section 5 some preliminary results of a global analysis are presented.

2. SPACECRAFT MODEL

Coordinate frames For the purpose of the present analysis, the following reference systems are adopted.

- Earth Centered Inertial reference axes (ECI). The origin of these axes is in the Earth's centre. The X-axis is parallel to the line of nodes. The Z-axis is parallel to the Earth's geographic north-south axis and pointing north. The Y-axis completes the right-handed orthogonal triad.
- Orbital Axes (X_0, Y_0, Z_0). The origin of these axes is in the satellite centre of mass. The X-axis points to the Earth's centre; the Y-axis points in the direction of the orbital velocity vector. The Z-axis is normal to the satellite orbit plane.
- Satellite body axes. The origin of these axes is in the satellite centre of mass; the axes are assumed to coincide with the body's principal inertia axes.

In this paper only the case of a spacecraft in a circular orbit is considered; the (constant) orbital angular rate will be denoted by ω_0. In the following the unit vectors corresponding to the orbital axes will be denoted with e_x, e_y and e_z respectively, with the superscript ^{o} (^{b}) when considering the components of the unit vectors along the orbital (body) axes.

Dynamics The attitude dynamics of a spacecraft subject to gravity gradient can be expressed in the body frame as (Wertz, 1978)

$$I\dot{\omega} = S(\omega)I\omega + 3\omega_0^2 S(Ie_x^b)e_x^b + T_{coils} + T_{dist} \tag{1}$$

where $\omega \in \mathbb{R}^3$ is the vector of spacecraft angular rates, $I = \mathrm{diag}[I_x, I_y, I_z] \in \mathbb{R}^{3\times 3}$ is the inertia matrix, $S(\omega)$ is given by

$$S(\omega) = \begin{bmatrix} 0 & \omega_z & -\omega_y \\ -\omega_z & 0 & \omega_x \\ \omega_y & -\omega_x & 0 \end{bmatrix}, \tag{2}$$

$T_{coils} \in \mathbb{R}^3$ is the vector of external torques induced by the magnetic coils and $T_{dist} \in \mathbb{R}^3$ is the vector of external disturbance torques.

Relative kinematics Dealing with the dynamics of an Earth pointing satellite, the focus is on the *relative* kinematics rather than on the inertial kinematics. We therefore consider the attitude of the spacecraft with respect to the (rotating) orbital axes. The attitude kinematics will described in terms of the four Euler parameters (or quaternions, see, *e.g.*, Wertz (1978)), which lead to the following representation for the relative attitude kinematics

$$\dot{q} = \tilde{W}(q)\omega_r \tag{3}$$

where $q = [q_1\ q_2\ q_3\ q_4]^T = [q_r^T\ q_4]^T$ is the vector of unit norm ($q^T q = 1$) Euler parameters,

$$\tilde{W}(q) = \frac{1}{2}\begin{bmatrix} q_4 & -q_3 & q_2 \\ q_3 & q_4 & -q_1 \\ -q_2 & q_1 & q_4 \\ -q_1 & -q_2 & -q_3 \end{bmatrix} \tag{4}$$

and $\omega_r = \omega - \omega_t = \omega + \omega_0 e_z^b$ is the satellite angular rate relative to the orbital axes, in body frame. Letting $A(q)$ the attitude matrix relating the orbital and the body frames, one has that

$$e_x^b = A(q)e_x^o = A(q)\begin{bmatrix}1\\0\\0\end{bmatrix} \tag{5}$$

and similarly for e_y^b,e_z^b. Finally, note that $\bar{q} = [0\ 0\ 0\ 1]^T$ represents the attitude equilibrium to be stabilized and that $A(q) = \mathcal{I}_3$ (where $\mathcal{I}_3$ is the identity matrix of dimension 3) for $q = \pm\bar{q}$.

Magnetic coils The magnetic attitude control torques are generated by a set of three magnetic coils, aligned with the spacecraft principal inertia axes, which generate torques according to the law

$$T_{coils} = m_{coils} \times \tilde{b}(t) = S(\tilde{b}(t))m_{coils}, \tag{6}$$

where $\times$ denotes the vector cross product, $m_{coils} \in \mathbb{R}^3$ is the vector of magnetic dipoles for the three coils, $\tilde{b}(t) \in \mathbb{R}^3$ is the vector formed with the components of the Earth's magnetic field in the body frame of reference. Note that the vector $\tilde{b}(t)$ can be obtained from the magnetic field vector $\tilde{b}_0(t)$ expressed in the inertial coordinates through the attitude matrix $A(q)$, namely

$$\tilde{b}(t) = A(q)\tilde{b}_0(t), \tag{7}$$

and that the orthogonality of $A(q)$ implies $\|\tilde{b}(t)\| = \|\tilde{b}_0(t)\|$. Since $S(\tilde{b}(t))$ is structurally singular, as mentioned in the Introduction, magnetic actuators do not provide full controllability of the system at each time instant. In particular, it is easy to see that rank$\left(S(\tilde{b}(t))\right) = 2$ (since $\|\tilde{b}_0(t)\| \neq 0$ along all orbits of practical interest for magnetic control) and that the kernel of $S(\tilde{b}(t))$ is given by the vector $\tilde{b}(t)$ itself, *i.e.*, at each time instant it is *not* possible to apply a control torque along the direction of $\tilde{b}(t)$.

If a preliminary feedback of the form

$$m_{coils} = \frac{1}{\|\tilde{b}_0(t)\|^2} S^T(\tilde{b}(t))u \tag{8}$$

is applied to the system, where $u \in \mathbb{R}^3$ is a new control vector, the overall dynamics can be written as

$$\begin{aligned} \dot{q} &= \tilde{W}(q)\omega_r \\ I\dot{\omega} &= S(\omega)I\omega + 3\omega_0^2 S(Ie_x^b)e_x^b + \Gamma(t)u + T_{dist} \end{aligned} \tag{9}$$

where $\Gamma(t) = S(b(t))S^T(b(t)) \geq 0$ and $b(t) = \frac{1}{\|\tilde{b}_0(t)\|}\tilde{b}(t) = \frac{1}{\|\tilde{b}(t)\|}\tilde{b}(t)$. Similarly, define $\Gamma_0(t) = S(b_0(t))S^T(b_0(t)) \geq 0$, and $b_0(t) = \frac{1}{\|\tilde{b}_0(t)\|}\tilde{b}_0(t)$.

As for the geomagnetic field, note that (see Psiaki (2001)) a dipole approximation of the Earth's magnetic field, under the assumptions of no Earth rotation and no orbit precession, yields the following periodic model for the magnetic field vector, expressed in orbit coordinates:

$$\tilde{b}_0(t) = \frac{\mu_f}{a^3}\begin{bmatrix} 2\sin(\omega_0 t)\sin(i_m) \\ \cos(\omega_0 t)\sin(i_m) \\ \cos(i_m) \end{bmatrix} \tag{10}$$

where $\mu_f = 7.9\ 10^{15}$ Wb m is the dipole strength, a is the orbit semimajor axis and i_m is the orbit's inclination with respect to the geomagnetic equator.

3. STATE FEEDBACK STABILIZATION

In this Section the general stabilisation result for a spacecraft with magnetic actuators given in Lovera and Astolfi (2006) for the case of full state feedback (attitude and rate) is recalled. More precisely, an almost globally convergent adaptive PD-like control law for Earth pointing magnetic attitude regulation is considered. The derivation of the control law is based on the following preliminary result.

Proposition 1. Consider the system (9) and the control law

$$u = -\varepsilon k_v \omega_r. \tag{11}$$

Let

$$\bar{\Gamma}_0 = \lim_{T\to\infty} \frac{1}{T}\int_0^T \Gamma_0(t)dt.$$

Supposing that $0 < \bar{\Gamma}_0 < \mathcal{I}_3$, then for all $\varepsilon > 0$ and $k_v > 0$ there exists $\bar{t} > 0$ such that for all $t > \bar{t}$

$$\bar{\Gamma}(t) = \frac{1}{t}\int_0^t \Gamma(\tau)d\tau > 0. \tag{12}$$

Proof. See Lovera and Astolfi (2006). ◁

The above proposition ensures that for sufficiently small angular rates the system (9) has "average" controllability properties as expressed by the full rank of the matrix $\bar{\Gamma}$. This fact allows the application of averaging theory (see Khalil (2001) for details) for the derivation of the control law studied in this paper, which is defined in the following Proposition.

Proposition 2. Consider the system (9) and the control law

$$u = \begin{cases} -\varepsilon k_v \omega_r & t \leq \bar{t} \\ -\hat{\Gamma}_{av}^{-1}(\varepsilon^2 k_p q_r + \varepsilon k_v \omega_r) & t > \bar{t} \end{cases} \tag{13}$$

where

$$\dot{\hat{\Gamma}}_{av} = \frac{1}{t}\Gamma - \frac{1}{t}\hat{\Gamma}_{av}, \quad t > 0 \tag{14}$$

and

$$\hat{\Gamma}_{av}(0) = \Gamma(0). \tag{15}$$

Then there exist $\varepsilon^\star > 0$, $k_p > 0$, $k_v > 0$ such that for any $0 < \varepsilon < \varepsilon^\star$ the control law renders the equilibrium $(q, \omega_r) = (\bar{q}, 0)$ of the closed loop system (9),(13), (14) locally exponentially stable. Moreover, all trajectories of the closed loop system (9),(13), (14) converge to the points $(q, \omega_r) = (\pm\bar{q}, 0)$.

Proof. See Lovera and Astolfi (2006). ◁

Proposition 2 shows that for magnetic attitude control the proportional and derivative actions must meet the scaling condition defined by averaging to guarantee closed-loop stability. Therefore, this result provides a useful guideline for the design of magnetic controllers in practical cases. Unfortunately, the choice of ε cannot be carried out on the basis of Proposition 2 only, but requires some additional methods and tools, which will be discussed in the following Sections. In particular, in order to deal with the periodically forced (*i.e.*, nonautonomous) nature of the closed-loop system, Floquet theory will be used in Section 4 for the local analysis (*i.e.*, based on the linear approximation of the closed-loop system around the equilibrium $(\bar{q}, 0)$) while a fully non-linear investigation will be carried out in Section 5.

In the following we will consider a spacecraft with an inertia matrix given by $I = \mathrm{diag}[5, 60, 70]$ kg m^2, operating in a near polar (87^o inclination) orbit with an altitude of 450 km and a corresponding orbit period of about 5600 s. Note that the first element of the inertia matrix is much smaller than the other two: such an inertia matrix is representative of a small satellite with a long gravity gradient boom along the x axis (see, *e.g.*, Wisniewski and Blanke (1999)). As for the control law, the considered parameters are given by $\varepsilon = 0.001$, $k_p = 500$ (A m^2), $k_v = 200$ A m^2/(rad/s).

4. LOCAL STABILITY ANALYSIS

In this Section the local stability of the closed-loop attitude equilibrium is analysed using a numerical approach. We consider the proposed model (9),(13),(14) neglecting the initial damping part (*i.e.*, only the second control law in (13)) is used, with Γ_{av} obtained as the asymptotic solution of (14), thus obtaining the system

$$\begin{aligned} \dot{q} &= \tilde{W}(q)\omega_r \\ I\dot{\omega} &= S(\omega)I\omega + 3\omega_0^2 S(Ie_x^b)e_x^b - \Gamma(t)\hat{\Gamma}_{av}^{-1}(\varepsilon^2 k_p q_r + \varepsilon k_v \omega_r). \end{aligned} \tag{16}$$

The system has the quaternion norm $q^T q$ as an invariant of motion, so numerical drift towards manifolds where $q^T q = \text{const} \neq 1$ can be observed in simulation. Instead of eliminating one variable, a damping term orthogonal to the 4-dim sphere $q^T q = 1$ is added to the kinematic equation. Therefore, equation (16) is replaced with

$$\dot{q} = W(q)\omega_b + (1 - q^T q)q.$$

In order to analyze the system with bifurcation analysis techniques (using packages as MatCont (Dhooge et al., 2003) or AUTO (Doedel et al., 2007)), the system is made autonomous, by adding the nonlinear oscillator

$$\begin{aligned} \dot{\alpha} &= \alpha - \omega_0\beta - (\alpha^2 + \beta^2)\alpha, \\ \dot{\beta} &= \omega_0\alpha + \beta - (\alpha^2 + \beta^2)\beta. \end{aligned} \tag{17}$$

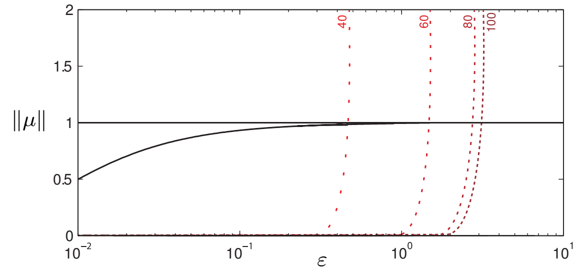

Fig. 1. Floquet multipliers associated with the periodic solution $\bar{x}(t)$ computed for several values of NTEST (40, 60, 80, and 100). Only the red multiplier is sensible to NTST, denoting its inaccuracy for low NTST or high ε.

Starting at the point $(\alpha, \beta) = (1, 0)$, we have $\alpha = \cos(\omega_0 t)$ and $\beta = \sin(\omega_0 t)$, so the additional states α and β can be used to eliminate the periodic time dependence from (10). For ease of notation, the full autonomous system (equations (16),(17)) is denoted by

$$\dot{x} = F(x, \varepsilon), \quad x = [q, \omega_r, \alpha, \beta] \in \mathbb{R}^9. \tag{18}$$

Note that the attitude equilibrium of the nonautonomous system is now a limit cycle of the new autonomous system, hereafter denoted by $\bar{x}(t) = [\bar{q}, 0, \cos t, \sin t]$.

As a first approach to the (local) stability of the limit cycle $\bar{x}(t)$ for system (18), the periodic solution was continued for increasing ε. For this, the considered system has been implemented in MatCont, which automatically discretizes the considered solution through orthogonal collocation techniques (see, *e.g.*, de Boor and Swartz (1973); Ascher et al. (1995)). Orthogonal collocation makes use of an adaptive mesh subdividing the time period into NTEST subintervals, in which the solution is approximated by polynomials of NCOL degree. In so doing the 9-dimensional boundary value problem is rewritten as an 9*(NTEST NCOL +1)-dimensional algebraic problem, that can be continued with respect to a parameter (say ε) (see Allgower and Georg (2000); Deuflhard et al. (1987); Meijer et al. (2009) for details). To compute the tangent direction to the ε-branch of solutions, it is necessary to compute the monodromy matrix M, such that $v(1) = Mv(0)$, where $\dot{v}(t) = TJ(\bar{x}(t))v(t)$ is the linearized dynamics in the neighborhood of the limit cycle $\bar{x}(t)$. Thus, the Floquet multipliers μ_i of the limit cycle are obtained (with great precision, at least for the largest one) as a by-product of the continuation. Note that one of the eigenvalues of M must be equal to $+1$ (the others being the Floquet multipliers), and verification of this condition along the continuation guarantees the accuracy of the computation.

In Figure 1 the multipliers associated with the periodic solution $\bar{x}(t)$ are reported, for different values of mesh dimension NTEST. As can be seen from the figure, all multipliers but one are not sensible to NTEST, while a real multiplier (very small for small ε), becomes unstable with increasing ε. However, the instability occurs at larger and larger values of ε if NTEST is increased. In view of this, the instability can be classified as a numerical artifact (the same computation made with NTEST = 1000 makes the destabilizing multiplier exit the unit circle at $\varepsilon \sim 47$). To better understand this phenomenon, the eigenfunction associated with the diverging multiplier has

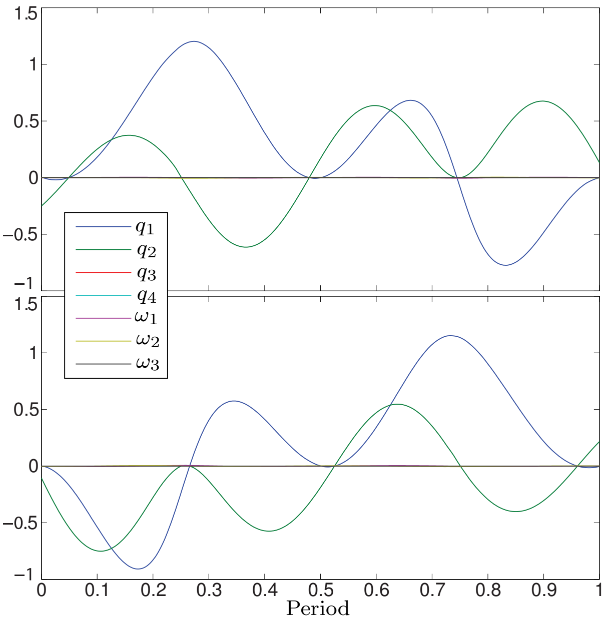

Fig. 2. Real and imaginary parts of the eigenfunction associated with the complex conjugate multipliers nearest to the stability boundary, for $\varepsilon = 0.1$, $\mu_{1,2} = -0.7522 \pm 0.5509i$ ($\|\mu_{1,2}\| = 0.9324$)).

been computed, by constructing the null-space of

$$\begin{cases} \dot{v}(t) - A(t)v(t) = 0, \ t \in [0, T], \\ \mu v(T) - v(0) = 0, \end{cases}$$

with the normalization equation ($\int_0^T \langle v(t), v(t) \rangle dt = 1$), using Gauss collocation and bordering techniques (Doedel et al., 2003; Della Rossa et al., to appear). Bordering allows to further test the accuracy of the computed pair multiplier-eigenfunction, providing a residual value that approaches 0 the more the computation is correct. We could therefore check that the residual increases (even by 4 or 5 orders of magnitude) as soon as the computed multiplier becomes greater than 10^{-9}. This fact confirms that the obtained instability is only a numerical artifact. Moreover, the inspection of the eigenfunction shows that there are high frequency oscillations (with large magnitude on the q_1 and q_2 directions), with frequency that grows with ε. This fact explains why a larger NTST is necessary to accurately compute the multipliers for large values of ε.

The obtained results allow to rule out loss of local stability up to very large values of ε. On the other hand, in Figure 1 it is possible to see a pair of complex conjugate multipliers reaching the stability boundary if ε increases. In Figure 2 the real and imaginary parts of the eigenfunctions (*i.e.*, the basis of the eigenspace) associated with this complex multiplier pair are shown (again, the q_1 and q_2 components are dominant). Perturbations given in the directions generated with this basis are associated with the slowest transients. Notice that, even if those two multipliers don't lead to stability loss, their absolute value is close to one ($\|\mu\| > 0.9$ if $\epsilon > 0.09$). We can therefore deduce that perturbations along the q_1 and q_2 directions are the ones that can more easily take to alternative asymptotic regimes, if existent, as will be discussed in the next section. Note that perturbations along the q_1 and q_2 directions amount to rotations around the roll and yaw axes (recall the definition of the orbital reference frame given in Section 2), which, for the considered orbit inclination, correspond to the non instantaneously controllable axes. The sensitivity of the feedback system to such perturbations is therefore easily explained. The pitch (orbit normal) axis, on the other hand, is locally instantaneously controllable, so it turns out to be less sensitive to perturbations.

5. GLOBAL ANALYSIS

A careful analysis of the basin of attraction for the attitude equilibrium $\bar{x}(t)$ calls for the construction of a two-parameter map in which both ε and the initial condition are varied, with randomized initial conditions $x(0) = \bar{x}(0) + \Delta x$. Carrying out such an analysis is computationally hard, since, as shown in the previous Section, the spacecraft attitude dynamics is characterised by a wide frequency separation between the closed-loop transients and the period of orbital revolution. In the following some preliminary results in this direction are presented and discussed. Recall that in the simulation of model (18) the initial damping phase (aimed at reducing the relative velocity ω_r) is neglected, so that we consider initial conditions with sufficiently small $|\omega_r|$.

First of all it was noticed that if ε is sufficiently small (say $\varepsilon < 0.005$), all the randomized tests confirm the result presented in Proposition 2. If now one considers a larger value for ε (*e.g.*, $\varepsilon = 0.01$), initial conditions with a small perturbation magnitude $\|\Delta x\|$ belong to the basin of attraction of the attitude equilibrium, while farther initial conditions lead to a different attractor (see the simulation shown in Figure 3). Note that, as shown in the previous section, in order to guarantee convergence to the desired equilibrium it is not necessary that the perturbation Δx is generally small, but it should be small in the q_1 and q_2 components. A projection in the angular rate of the attractor reached in Figure 3 is shown in Figure 4. The shown trajectory corresponds to one spacecraft orbit: notice, as expected, that we have high frequency oscillations. Computing the Lyapunov exponents of the attractor (Wolf et al., 1985) we obtain that the first one takes value $L_1 = 0.0089$ ($L_2 = -0.0007$, $L_3 = -0.0013$), confirming that we are in presence of a (weakly) chaotic behavior. For an even larger value of ε ($\varepsilon = 0.1$) a similar result is obtained even starting from a point nearer to the trivial equilibrium ($\|\Delta x\| = 10^{-5}$). The oscillations have both larger amplitude and higher frequency. Nevertheless, the computed first Lyapunov exponent is smaller ($L_1 = 0.0006$, $L_2 = -0.000002$, $L_3 = -0.0005$), and the attractor is more regular, all indications that the chaotic behavior is weaker than in the previous case.

6. CONCLUDING REMARKS

In this paper the dynamics of an Earth pointing spacecraft equipped with magnetic actuators operating under a static attitude and rate feedback control law designed using averaging theory has been considered. The problem of determining the asymptotic behavior of the closed-loop system as a function of the averaging scaling parameter has been analyzed, using numerical continuation methods. The results provide a useful complement to the existing theory based on averaging techniques as they allow an assessment

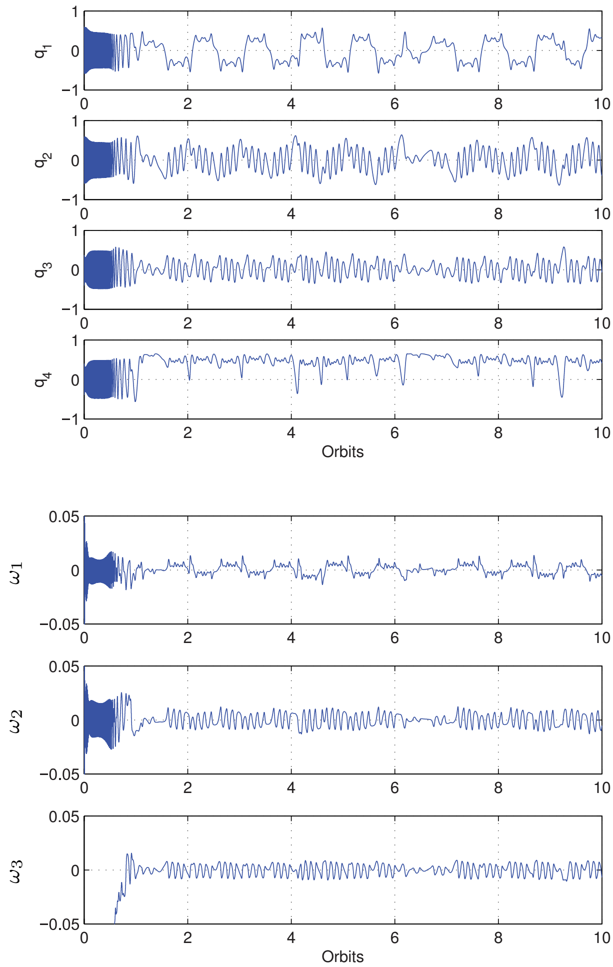

Fig. 3. Time evolution of quaternion (upper panels) and angular rate (lower panels) recovery from an initial condition far from the desired asymptotic behavior ($\varepsilon = 0.01$, $\|\Delta x\| = 10^{-3}$).

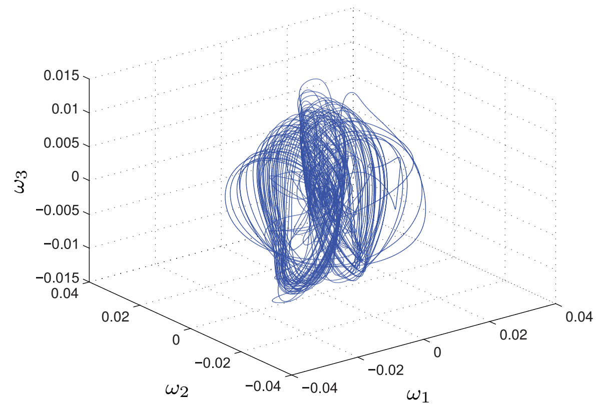

Fig. 4. Asymptotic behavior obtained with $\varepsilon = 0.01$ departing from an initial condition far from the desired asymptotic behavior.

of the range of values of the scaling parameter for which the closed-loop system exhibits the desired equilibrium as sole asymptotic behavior and a catalogue of other possible attractors for the range of practical interest of the parameter.

REFERENCES

Allgower, E. and Georg, K. (2000). *Numerical Continuation Methods: An Introduction*. Berlin.

Arduini, C. and Baiocco, P. (1997). Active magnetic damping attitude control for gravity gradient stabilised spacecraft. *Journal of Guidance and Control*, 20(1), 117–122.

Ascher, U., Mattheij, R., and Russell, B. (1995). *Numerical Solution of Boundary Value Problems for Ordinary Differenital Equations*. Philadelphia.

Bhat, S. and Dham, A. (2003). Controllability of spacecraft attitude under magnetic actuation. In *IEEE Conference on Decision and Control, Maui, Hawaii, USA*.

Chen, L. and Liu, Y. (2002). Chaotic attitude motion of a magnetic rigid spacecraft and its control. *International Journal of Non-Linear Mechanics*, 37(3), 493–504.

Damaren, C.J. (2002). Comments on "Fully magnetic attitude control for spacecraft subject to gravity gradient". *Automatica*, 38(12), 2189.

de Boor, C. and Swartz, B. (1973). Collocation at gaussian points. *SIAM Journal of Numerical Analysis*, 10, 582606.

Della Rossa, F., Bergamasco, M., and Lovera, M. (2012). Bifurcation analysis of the attitude dynamics for a magnetically controlled spacecraft. In *51st IEEE Conference on Decision and Control, Maui, USA*.

Deuflhard, P., Fiedler, B., and Kunkel, P. (1987). Efficient numerical pathfollowing beyond critical points. *SIAM Journal of Numerical Analysis*, 24, 912927.

Dhooge, A., Govaerts, W., and Kuznetsov, Yu.A. (2003). MATCONT: A MATLAB package for numerical bifurcation analysis of ODEs. *ACM Trans. Math. Software*, 29(2), 141–164. URL `http://doi.acm.org/10.1145/779359.779362`. `http://sourceforge.net/projects/matcont`.

Doedel, E.J., Champneys, A.R., Dercole, F., Fairgrieve, T.F., Kuznetsov, Yu.A., Oldeman, B., Paffenroth, R.C., Sandstede, B., Wang, X.J., and Zhang, C.H. (2007). AUTO-07p: Continuation and bifurcation software for ordinary differential equations. Department of Computer Science, Concordia University, Montreal, QC.

Doedel, E.J., Govaerts, W., and Kuznetsov, Yu.A. (2003). Computation of periodic solution bifurcations in ODEs using bordered systems. *SIAM J. Numer. Anal.*, 41(2), 401–435. doi: http://dx.doi.org/10.1137/S0036142902400779. URL `http://epubs.siam.org/sam-bin/dbq/article/40077`.

Fujii, H., Ichiki, W., Suda, S., and Watanabe, T. (2000). Chaos analysis of librational control of gravity-gradient satellite in elliptic orbit. *Journal of Guidance, Control and Dynamics*, 23(1), 145–146.

Khalil, H. (2001). *Nonlinear systems*. Prentice Hall.

Kuang, J., Tan, S., and Leung, A. (2002). Chaotic attitude tumbling of an asymmetric gyrostat in a gravitational field. *Journal of Guidance, Control and Dynamics*, 25(4), 804–814.

Lovera, M. and Astolfi, A. (2004). Spacecraft attitude control using magnetic actuators. *Automatica*, 40(8), 1405–1414.

Lovera, M. and Astolfi, A. (2006). Global magnetic attitude control of spacecraft in the presence of gravity gradient. *IEEE Transactions on Aerospace and Electronic Systems*, 42(3), 796–805.

Lovera, M., De Marchi, E., and Bittanti, S. (2002). Periodic attitude control techniques for small satellites with magnetic actuators. *IEEE Transactions on Control Systems Technology*, 10(1), 90–95.

Lowenberg, M. and Menon, P. (2007). An analysable nonlinear criterion for clearance of flight control laws. In *AIAA Guidance, Navigation and Control Conference and Exhibit, Hilton Head, USA*.

Della Rossa, F., De Witte, V., Govaerts, W., and Kuznetsov, Y. (to appear). Numerical periodic normalization for codim 2 bifurcations of limit cycles - computational formulas, numerical implementation, and examples. *SIAM Journal on Applied Dynamical Systems*.

Mehra, R. and Prasanth, R. (1998). Application of nonlinear global analysis and system identification to aircraft-pilot coupled oscillations. In *1998 IEEE International Conference on Control Applications, Trieste, Italy*.

Meijer, H.G.E., Dercole, F., and Oldeman, B.E. (2009). Numerical bifurcation analysis. In R.A. Meyers (ed.), *Encyclopedia of Complexity and System Science*, 6329–6352.

Psiaki, M. (2001). Magnetic torquer attitude control via asymptotic periodic linear quadratic regulation. *Journal of Guidance, Control and Dynamics*, 24(2), 386–394.

Silani, E. and Lovera, M. (2005). Magnetic spacecraft attitude control: A survey and some new results. *Control Engineering Practice*, 13(3), 357–371.

Wang, P. and Shtessel, Y. (1998). Satellite attitude control using only magnetic torquers. In *AIAA Guidance, Navigation, and Control Conference and Exhibit, Boston, USA, 1998*.

Wertz, J. (1978). *Spacecraft attitude determination and control*. D. Reidel Publishing Company.

Wisniewski, R. and Blanke, M. (1999). Fully magnetic attitude control for spacecraft subject to gravity gradient. *Automatica*, 35(7), 1201–1214.

Wisniewski, R. and Stoustrup, J. (2004). Periodic H_2 Synthesis for Spacecraft Attitude Control with Magnetorquers. *Journal of Guidance, Control and Dynamics*, 27(5), 874–881.

Wolf, A., Swift, J.B., Swinney, H.L., and Vastano, J.A. (1985). Determining Lyapunov exponents from a time series. *Physica D*, 16, 285–317.

Zanchettin, A. and Lovera, M. (2011). H_∞ attitude control of magnetically actuated satellites. In *IFAC World Congress, Milano, Italy*.